Microfluidic release of the rare cells captured by a filter with tapered holes

Feng Liang, Juan Peng, Jian Shi, Li Wang, Carole Aimé, Yong Chen

MNE 14 (2022) 100119

Contents lists available at ScienceDirect

Micro and Nano Engineering

journal homepage: www.sciencedirect.com/journal/micro-and-nano-engineering

Microfluidic release of the rare cells captured by a filter with tapered holes

Feng Liang [a], Juan Peng [a], Jian Shi [b], Li Wang [b], Carole Aimé [a], Yong Chen [a,*]

[a] PASTEUR, Département de chimie, École normale supérieure, PSL University, Sorbonne Université, CNRS, 24 rue Lhomond, 75005 Paris, France
[b] MesoBioTech, 231 Rue Saint-Honoré, 75001 Paris, France

ARTICLE INFO

Keywords:
Microfluidic
Filter
Rare cells
Capture
Release

ABSTRACT

Rare cells such as circulating tumor cells and prenatal fetal cells can be captured by size-dependent filtration using a microfluidic device. Herein, we report a method to release the captured cells with the same microfluidic device which consisted of a microfabricated filter with tapered holes. When a cell containing flow passed through the filter, the cells could be blocked by the filter. Afterward, a reverse flow was applied to release the captured cells. To increase the efficiency of the capture and the release, a filter with tapered holes was used and micro-particles of sizes between smaller and large hole diameters were added into the reverse flow. We found that when the majority of the holes were blocked, the trans-filter flow resistance drastically increased and most of the captured cells could be released. As a proof of concept, ovarian cancer cells SKOV3 were used, showing a high release efficiency and remarkable viability of the collected cells.

1. Introduction

Rare cells such as circulating tumor cells (CTCs) and prenatal fetal cells are valuable biomarkers that can now be captured from billions of red and white blood cells in a few milliliters of a peripheral blood sample [1]. Compared to the other methods including affinity-based recognition [2–4], inertia-based separation [5,6], electrochemistry-based detection [7,8], nanostructure-based capture [9,10], the size-based filtration [11–14] is perhaps the simplest and most direct. This method relies mainly on the size and deformability differences between the rare cells and the blood cells. Once captured, the cells could be enumerated and characterized thoroughly with the downstream analytic methods.

Previously, we developed a method to capture CTCs using a microfluidic device with an integrated filter with tapered holes [15]. By using a filter with small hole diameter of 6.5 μm, a flow rate of 0.5 mL/min, and different tumor cell lines, a capture efficiency as high as 98% could be reached. Remarkably, up to 95% of the captured cells were alive for proliferation on the filter. In order to facilitate the downstream analyses, we developed in this work a method to release the captured cells by using the same device. We firstly performed the cell using the same method as previously reported. Then, we applied a reversed flow with a solution containing micro-particles to block the holes of the filter where no cell was captured. We found that when the majority of the holes were blocked, the trans-filter flow resistance drastically increased and 92.2% of cells could be recovered after capture and release. We show that its release efficiency depends on the percentage of blocked holes and that the released cells presented a good cell viability.

2. Materials and methods

2.1. Microfluidic system

Fig. 1(a) shows the microfluidic system used in this work, which consists of a plastic microfluidic device with an integrated tapered-hole filter, a high precision air pressure generator (from MesoBioTech, France), four falcon tubes, four electromagnetic valves, and silicone pipelines. All fluidic connections were done via standard Luer connectors and the pressure regulation was achieved with Arduino board integrated inside the air pressure generator. When the system was used for cell capture, valve 1 and valve 4 were switched on and the cell suspension in tube 1 was pushed out by air pressure, entered into the microfluidic device from inlet 1 to outlet 2, and finally went to tube 4. In such a way, cells could be captured by the filter, as shown in Fig. 1(b). When the system was used for cell release, valve 2 and valve 4 were switched on and the two other valves were switched off. A polystyrene micro-particle containing solution (from Sigma, France) in tube 3 was extruded out by air pressure, entered into the microfluidic device from inlet 2 to outlet 1, and finally went to tube 2 (Fig. 1(c)).

* Corresponding author.
E-mail address: yong.chen@ens.psl.eu (Y. Chen).

https://doi.org/10.1016/j.mne.2022.100119
Received 4 October 2021; Received in revised form 10 January 2022; Accepted 26 February 2022
Available online 2 March 2022

2.2. Microfilter with tapered holes

Filters of 30 μm thickness and tapered holes of 6.5 μm and 17 μm diameters were provided by MesoBioTech. These filters were bounded to a 100 μm thick and 9 mm inner and 13 mm outer diameter ring for easy handing (Fig. 2(a-b)). To avoid cell adhesion during capture, they were coated with PLL (20)-g[3.5]- PEG(2) (Susos) for 1 h in 37 °C with a concentration of 0.1 mg/mL.

2.3. Cell culture, immunostaining, and dehydration

SKOV3 cells were cultured in RPMI-1640 medium containing 10% FBS (fetal bovine serum, Sigma, France), penicillin (100 U/mL), and streptomycin (100 U/mL) under 37 °C and 5% CO_2 in a humidified atmosphere incubator. Before cell capture, cell nuclei were stained by Hoechst 33342 (ThermoFisher, France) for 30 min and then washed with PBS (phosphate buffer saline, Gibco, France) for 3 times. Fluorescence imaging of cell release was conducted on a Zeiss Observer Z1 fluorescence microscope (Fig. 2(d)). The cells release efficiency was calculated by the released cells number divided by the total captured cells number. Cells were fixed with 4% PFA (Paraformaldehyde, Gibco, France) for 15 min, dehydrated gradually in ethanol twice (50%, 60%, 70%, 80%, 90%, and 100%, each for 10 min), and dried in vacuum overnight.

2.4. Scanning electron microscopy (SEM) characterization

Samples were observed using a scanning electron microscope (TM3030, Hitachi, Japan) with an accelerating voltage of 15 kV. Before scanning electron microscopy observation, samples were coated with a 2 nm thick Au layer by sputtering.

2.5. Cell viability assessment

Cell viability was studied by live/dead assay. Briefly, 4 μM Calcein AM (Invitrogen, L3224) and 5 μM propidium iodide (Sigma-Aldrich, P4170) in PBS solution were added to the released cells collection for live and dead cell staining, respectively. After 30 min incubation at 37 °C and 5% CO_2, cells were analyzed with a fluorescence microscope, as described above.

3. Results and discussion

The filter we used consists of more than 2×10^5 tapered holes. During the cell capture, only a very small portion of the holes was blocked or partially blocked by the captured cells so that the flow resistance remained the same. With a revered flow of small flow rate, the trans-filter pressure generated forces on cells would not be sufficient. However, when the majority of the holes were blocked by micro-particles, the trans-filter pressure can be largely increased to generate hydrodynamic forces to push away the captured cells.

To estimate the cells release efficiency, we first calculated the trans-filter pressure with a constant flow, $\Delta P = 3\eta Q/Na^3$, where η is viscosity and Q is the flow rate of the liquid, N is the number of open holes and a is the hole radius [16]. For the zeroth-order approximation, the height of the holes was assumed to be infinitely small and the hole size was the small diameter of the tapered holes. Accordingly, the normalized flow resistance, r/r_p ($r_p = 3\eta/a^3$), as a function of the percentage of blocked holes can be plotted, as shown in Fig. 3(a). Interestingly, the flow resistance increases smoothly up to ~80% of the hole blockage and then varies drastically, suggesting that a huge flow resistance can be achived when the majority of the holes are blocked. This effect does not depend on the number and size of the holes nor the viscosity of the liquid. Experimentally, a constant flow rate can be easily achieved by using a motorized syringe pump. In this work, however, constant pressure was applied for simplicity, which makes the analysis slightly different. Now, the flow resistance is the resistance of the filter, r_f, plus that of the rest of the fluidic circuit, r_0. In our case, $r_0 \gg r_f$ when the majority of the holes were not blocked so that the trans-filter pressure is relatively small compared to the pressure drop of the rest of the fluidic circuit as shown in Fig. 3(b). However, when the majority of the holes were blocked, $r_0 \ll r_f$, which may result in high trans-filter pressure and thus large forces for the cell release (Fig. 3(c)).

In our experiments, a solution of 5×10^4 SKOV3 cells in a 10 mL culture medium was injected from inlet 1 into the microfluidic device and a pressure of 100 mbar was applied for the cell capture whose fluorescence images of Hoechst stained (blue) cells were shown in Fig. 4 (a,d). After stabilisation, a solution of micro-particles in PBS was

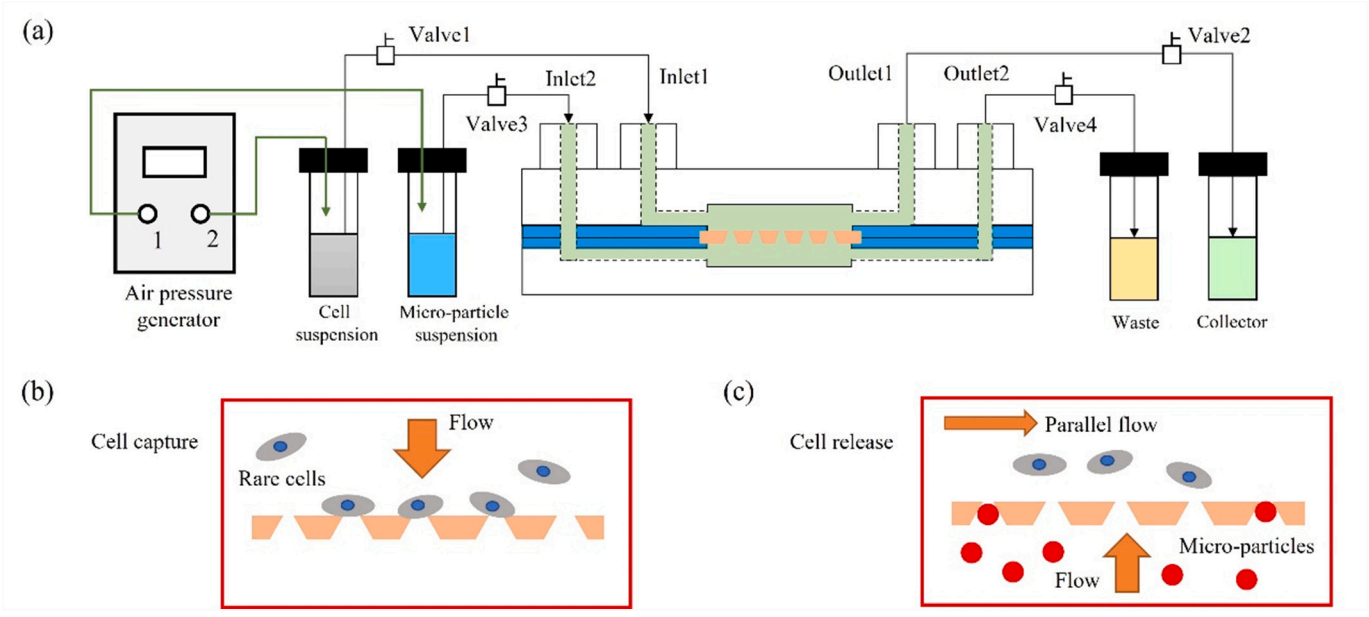

Fig. 1. (a) Schematic diagram of a microfluidic system for label-free cell capture and release. For cell capture, the cell suspension is introduced into the microfluidic device, and cells are isolated by the integrated tapered-hole filter (b, passage inlet 1 – outlet 2). For cell release, a micro-particles containing solution is introduced to block the open holes of the filter so that the trans-filter flow resistance and pressure will increase, and the captured cells can be released (c, passage inlet 2 – outlet 1).

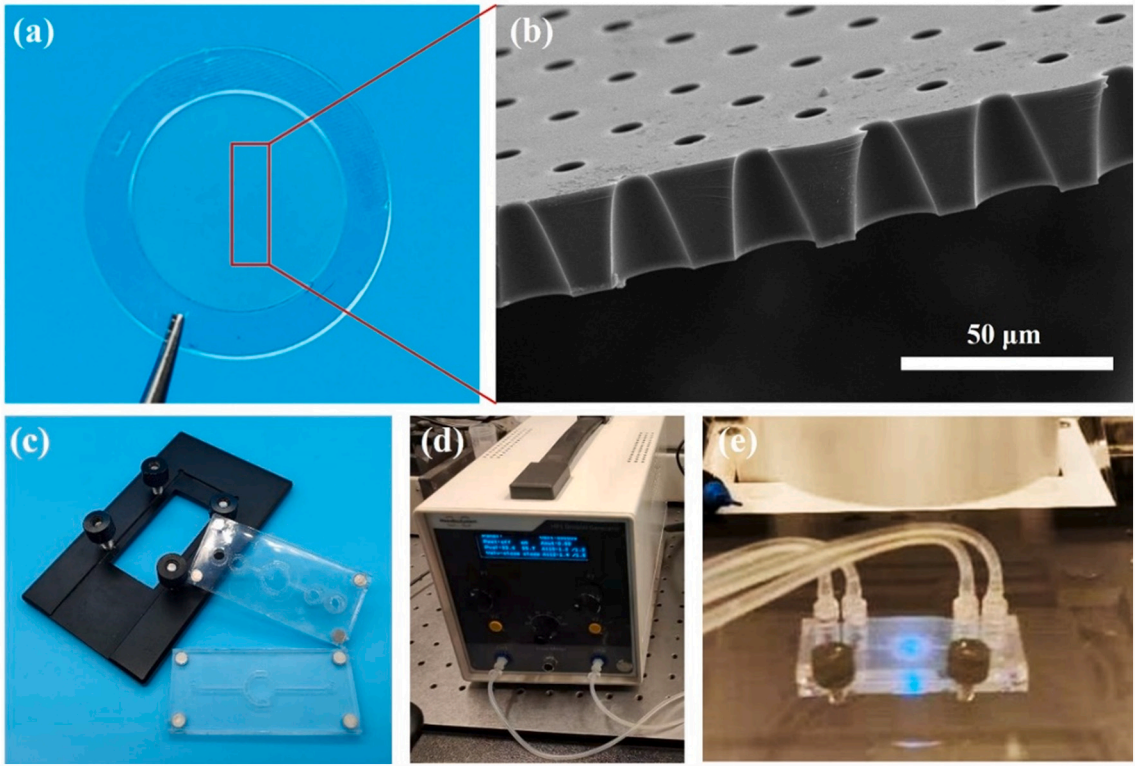

Fig. 2. (a) Photograph and (b) SEM image of the tapered-hole filter, (c) a microfluidic device and a clamp before assembling, (d) a high-precision air pressure generator, and (e) the assembled device with pipelines.

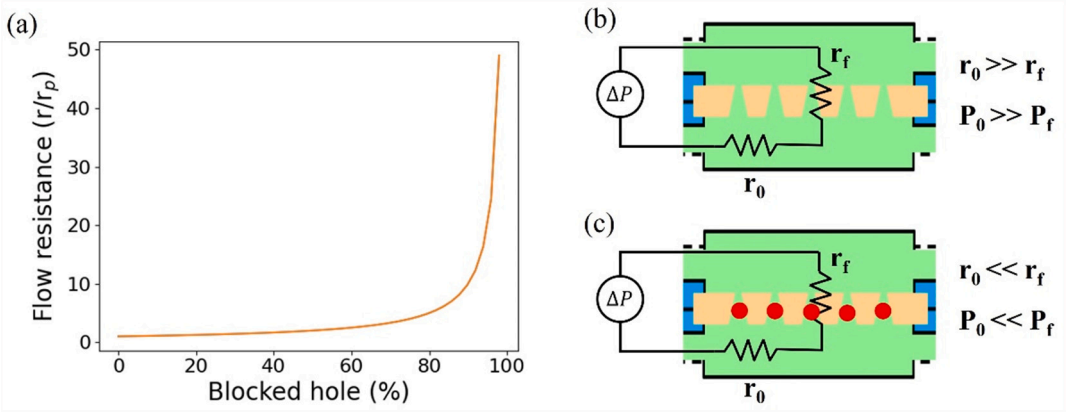

Fig. 3. (a) Numerical calculation of trans-filter flow resistance as a function of the percentage of blocked holes (r_p: flow resistance of single hole). Schematic diagram of differences in flow resistance and pressure of transfilter and fluidic circuit before (b) and after (c) holes blocked (r_0: flow resistance of the fluidic circuit, rf: trans-filter flow resistance, P_0: pressure drop of the fluidic circuit, P_f: transfilter pressure).

injected into the device from inlet 2 and a pressure of 100 mbar was applied. By enumerating the cells number on the filters after cell capture and release, the cell release efficiency could be evaluated and shown in Fig. 4(h). Fig. 4(b,c) and Fig. 4(e,f) showed fluorescence images of cells remained on the filters with 50% and 95% blocked holes, respectively. When 50% holes of the filter were blocked, only 51.3 ± 1.7% of the captured cells could be released (Fig. 4(b)). When the blocked holes percentage reached to 95%, however, there were still 33.1 ± 3.4% of the captured cells left on the filter (Fig. 4(e)). The reason is that with a constant pressure, the particle-blockage increased the trans-filter flow resistance but decreased the flow rate at the same time. It seems that most of the captured cells could be detached from the tapered hole but still stayed on the filter due to the low flow rate. Therefore, we applied additionally a tangent or parallel flow of PBS from inlet 1 to outlet 1 to flush the filter. As expected, the release efficiency of the filter with 50% blocked holes increased to 75.7 ± 1.9% (Fig. 4(c)), and that with 95% blocked holes reached 92.2 ± 0.6%(Fig. 4(f)) with a parallel flow under a pressure of 100 mbar. Only 7.8% of the total injected cells remained on the filter, probably due to the stronger cell adhesion. The SEM images of the filter after cell capture and release were shown in Fig. 4(g), where red and white arrows indicated cells and micro-particles, respectively.

The viability of the released cells is a significant factor. Different stresses on cells might be induced during the cell capture and release processes, including 1) filtration stress with a forward flow during cell capture, 2) release stress with a reverse flow during cell release, and 3) shear stress in the channels and pipelines. The filtration and the release flow stresses both depend on the transfilter pressure. By accurately controlling the flowrate, for example, the transfilter pressure would be

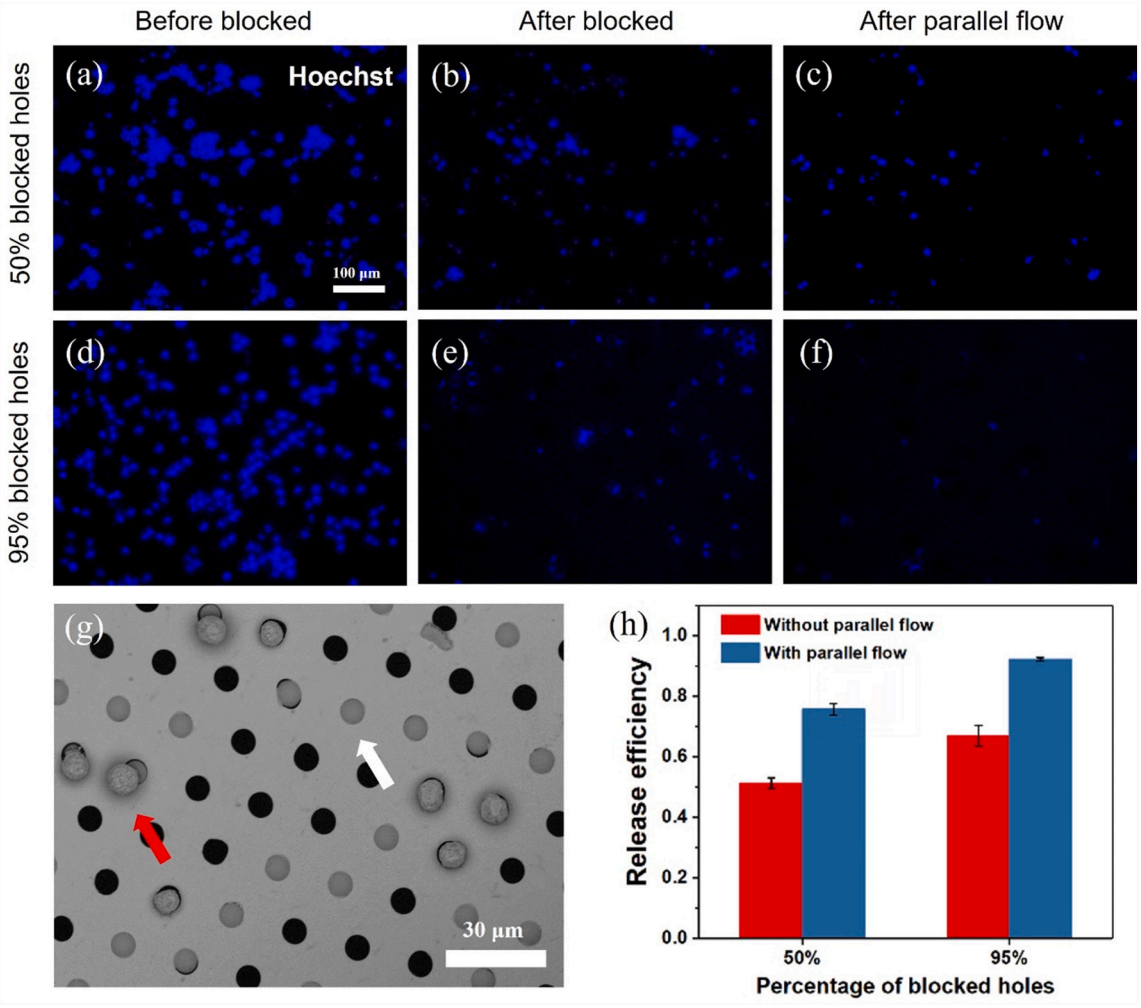

Fig. 4. Fluorescence images of the cells on the filter before (a, d) and after (b, c, e, f) release, showing that the release efficiency increases with the percentage of hole blockage and that the parallel flow (c, f) has a strong effect on the cell release. Cells were marked in blue with Hoechst. The SEM image (g) illustrates the blockage of the tapered holes by micro-particles (white arrows) and unreleased cells (Red arrows). (h) Release efficiency of 50% and 95% blocked holes, with and without parallel flow, respectively. (For interpretation of the references to colour in this figure legend, the reader is referred to the web version of this article.)

limited to reduce the cell damage effect. During the release with added micro-particles, the transfilter pressure increases, and the captured cells could be detached under a relatively low transfilter pressure. Our following results showed that the majority of detached cells were alive without significant damage.

To estimate the shear stress of the channel and pipelines, the geometry parameters can be used. Typically, a pipeline of length 1600 mm and diameter 1.6 mm was used to connect the cell source and the microfluidic device, and a rectangle channel of length 20 mm, width 0.5 mm, and height 0.5 mm was used to connect the inlet and the upper chamber. According to Hagen–Poiseuille's law, the flow resistance of the pipeline and the channel can be calculated [17] and we obtained a flow resistance of the upstream $R_s = 1.73 \times 10^{10}\ Pa \bullet s/m^3$ with a viscosity of water $\mu = 0.89\ mPa \bullet s$. The flow rate, $Q = \Delta P/R_s$, can then be calculated for a given pressure drop ΔP. With $\Delta P = 100$ mbar, a flow rate of $5.78 \times 10^{-7}\ m^3/s$ is obtained. Accordingly, shear stress of 24.71 Pa and 1.28 Pa is obtained for the channel and the pipeline [17,18]. The shear stress in the upper chamber of diameter 9 mm and height 1.2 mm can also be estimated, which is 4.29 Pa at the entrance and 0.24 Pa in the middle of the chamber, respectively. The above-estimated shear stresses should be small enough to prevent cell damage, explaining the resulted cell viability.

Experimentally, we evaluated the cell viability of the collected cells which were released with a 95% hole blockage. Calcein AM and propidium iodide were added to the collected cell suspension to stain live and dead cells respectively, indicating that 95.1 ± 0.8% of these cells were alive as shown in Fig. 5(a-d). We then cultured them to verify their proliferation ability and found twice cells number after incubation for 48 h due to the fact that the double time of SKOV3 cells was 48 h, as shown in Fig. 5(e-f). This demonstrated the viability of the proposed method, which did not cause significant cell damage during the whole process of the capture and release.

We would like to mention that this study is proof of the concept which has to be validated with clinic samples. It is true that the size and deformability of CTCs partially overlap with that of white blood cells (WBC). Nevertheless, most of WBCs and all red blood cells and platelets can easily pass the tapered filter under pressure. Under optimal conditions, the ratio of CTC to WBC of recovered cells after releasing should be much larger than that of a blood sample, which is in favor of downstream analyses such as PCR or sequencing after positive or negative sorting. Studies will be carried out along this line to further validate the potential of the present concept.

4. Conclusion

We demonstrated a simple yet efficient method for the release of microfilter captured cells by using a reverse flow with micro-particles. Typically, when 95% of the holes of the filter are blocked, a cell

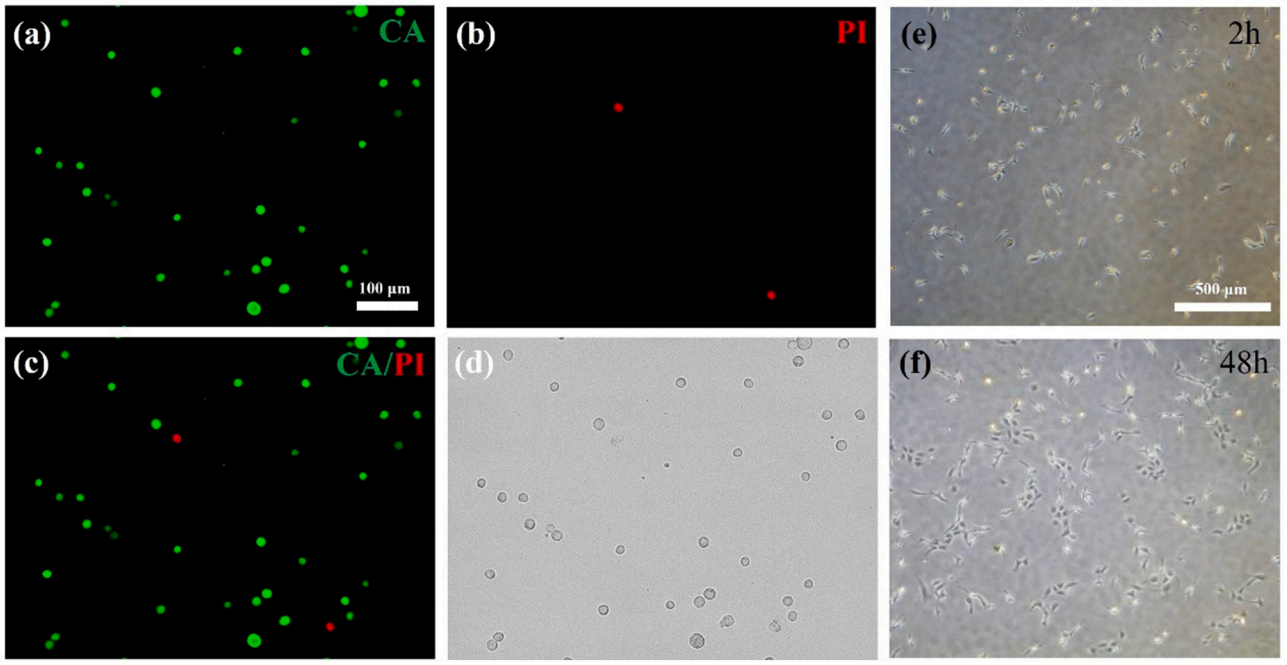

Fig. 5. (a-c) Live/dead fluorescence images of released SKOV-3 cells. (d) Bright-field image of the cells. (e, f) Bright-field images of released SKOV-3 cells after incubation for 2 h and 48 h, respectively, showing a proliferation behavior confirming again the cell viability.

release efficiency of 92.2% can be achieved. Furthermore, most of the released cells remained alive, which can be cultured for downstream analyses. The fluidic components used in this work, including microfilter, microfluidic device and controller, and microparticles, are all commercially available, making this method accessible for further investigations.

CRediT authorship contribution statement

Feng Liang: Conceptualization, Investigation, Writing-Original Draft. **Juan Peng**: Formal analysis. **Jian Shi**: Methodology, Validation. **Li Wang**: Resources. **Carole Aimé**: Resources. **Yong Chen**: Supervision, Writing- Reviewing and Editing.

Declaration of Competing Interest

None.

Acknowledgments

This work has received support from French National Research Agency (ANR-17-CE09-0017, ANR-10-IDEX-0001-02 PSL, and ANR-10-LABX-31), Région Ile-de-France (DIM-ELICIT), PSL-valorization (program pre-maturation), Carnot-IPGG, and European Commission Cost Action (BIONECA, CA 16122). Feng Liang is are grateful to the China Scholarship Council for grant of his PhD studies.

References

[1] V. Akpe, T.H. Kim, C.L. Brown, et al., Circulating tumour cells: a broad perspective [J], J. R. Soc. Interface 17 (168) (2020) 20200065.
[2] K. Chen, J. Amontree, J. Varillas, et al., Incorporation of lateral microfiltration with immunoaffinity for enhancing the capture efficiency of rare cells[J], Sci. Rep. 10 (1) (2020) 1–12.
[3] L. Zhao, C. Tang, L. Xu, et al., Enhanced and differential capture of circulating tumor cells from lung cancer patients by microfluidic assays using aptamer cocktail [J], Small 12 (8) (2016) 1072–1081.
[4] M. Deliorman, F.K. Janahi, P. Sukumar, et al., AFM-compatible microfluidic platform for affinity-based capture and nanomechanical characterization of circulating tumor cells[J], Microsyst. Nanoeng. 6 (1) (2020) 1–15.
[5] R. Nasiri, A. Shamloo, J. Akbari, et al., Design and simulation of an integrated centrifugal microfluidic device for CTCs separation and cell lysis[J], Micromachines 11 (7) (2020) 699.
[6] J. Zhou, A. Kulasinghe, A. Bogseth, et al., Isolation of circulating tumor cells in non-small-cell-lung-cancer patients using a multi-flow microfluidic channel[J], Microsyst. Nanoeng. 5 (1) (2019) 1–12.
[7] S.S. Wang, X.P. Zhao, F.F. Liu, et al., Direct plasmon-enhanced electrochemistry for enabling ultrasensitive and label-free detection of circulating tumor cells in blood [J], Anal. Chem. 91 (7) (2019) 4413–4420.
[8] P. Reokrungruang, I. Chatnuntawech, T. Dharakul, et al., A simple paper-based surface enhanced Raman scattering (SERS) platform and magnetic separation for cancer screening[J], Sensors Actuators B Chem. 285 (2019) 462–469.
[9] Z. Wang, N. Sun, M. Liu, et al., Multifunctional nanofibers for specific purification and release of CTCs[J], ACS Sens. 2 (4) (2017) 547–552.
[10] H. Xu, B. Dong, Q. Xiao, et al., Three-dimensional inverse opal photonic crystal substrates toward efficient capture of circulating tumor cells[J], ACS Appl. Mater. Interfaces 9 (36) (2017) 30510–30518.
[11] X. Ren, B.M. Foster, P. Ghassemi, et al., Entrapment of prostate cancer circulating tumor cells with a sequential size-based microfluidic chip[J], Anal. Chem. 90 (12) (2018) 7526–7534.
[12] A.F. Sarioglu, N. Aceto, N. Kojic, et al., A microfluidic device for label-free, physical capture of circulating tumor cell clusters[J], Nat. Methods 12 (7) (2015) 685–691.
[13] C. Lopes, P. Piairo, A. Chícharo, et al., HER2 expression in circulating tumour cells isolated from metastatic breast Cancer patients using a size-based microfluidic device[J], Cancers 13 (17) (2021) 4446.
[14] C. Yang, N. Zhang, S. Wang, et al., Wedge-shaped microfluidic chip for circulating tumor cells isolation and its clinical significance in gastric cancer[J], J. Transl. Med. 16 (1) (2018) 1–12.
[15] Y. Tang, J. Shi, S. Li, et al., Microfluidic device with integrated microfilter of conical-shaped holes for high efficiency and high purity capture of circulating tumor cells[J], Sci. Rep. 4 (1) (2014) 1–7.
[16] R. Holdich, et al., Pore design and engineering for filters and membranes, Phil. Trans. R. Soc. A 364 (2006) 161–174.
[17] K.W. Oh, K. Lee, B. Ahn, et al., Design of pressure-driven microfluidic networks using electric circuit analogy[J], Lab Chip 12 (3) (2012) 515–545.
[18] L. Wang, Z.L. Zhang, J. Wdzieczak-Bakala, et al., Patterning cells and shear flow conditions: convenient observation of endothelial cell remoulding, enhanced production of angiogenesis factors and drug response[J], Lab Chip 11 (24) (2011) 4235–4240.